CHEMISTRY OF MATERIALS
Cite This: Chem. Mater. 2019, 31, 3851−3862
Perspective
pubs.acs.org/cm

# Unraveling the Mechanisms of Thermal Quenching of Luminescence in $Ce^{3+}$-Doped Garnet Phosphors†

Yuan-Chih Lin,[‡] Marco Bettinelli,[§] and Maths Karlsson*,[‡]

[‡]Department of Chemistry and Chemical Engineering, Chalmers University of Technology, SE-412 96 Göteborg, Sweden
[§]Luminescent Materials Laboratory, Department of Biotechnology, University of Verona and INSTM, UdR Verona, 37134 Verona, Italy

**ABSTRACT:** The environmental and economic benefits of phosphor-converted white-light-emitting diodes (pc-WLEDs) have been increasingly appreciated in recent years. However, a significant challenge in this field pertains to a phenomenon known as thermal quenching, which takes place inside phosphors and leads to a pronounced reduction of the emission intensity under high-power light-emitting diode operation. The development of new, more thermally stable phosphors depends on a better understanding of the mechanisms underpinning thermal quenching in phosphors. Here we review the current understanding of thermal quenching mechanisms in $Ce^{3+}$-doped garnet phosphors, which are widely considered one of the most important families of phosphors for application in pc-WLEDs. In particular, we highlight key structural and dynamical properties, such as the coordination environment of the $Ce^{3+}$ ions, phonons and local vibrational modes, and structural and chemical defects, which are shown to correlate with phosphor performance. We also discuss the perspectives for future studies in this field in hopes of accelerating the development of new efficient phosphors featuring suppressed thermal quenching of luminescence.

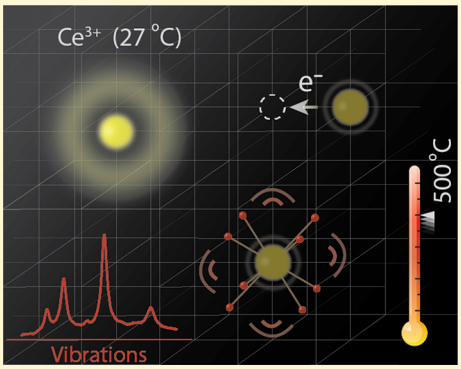


## 1. INTRODUCTION

The technology of phosphor-converted white-light-emitting diodes (pc-WLEDs) has been extensively integrated into our daily lives due to its environmentally friendly nature, robustness, and long lifetime. The most widely used type of pc-WLED is composed of an (In,Ga)N-based blue LED (emission wavelengths of 450−480 nm) that is used to excite either a layer of a yellow phosphor or a layer of a green and a red phosphor on top of the LED, so that the mixture of light generated by the phosphor layer and the blue light leaking through the phosphor layer creates white light (Figure 1a).[1−5] The phosphors usually consist of a crystalline host material doped with a small number of activator ions that serve as luminescent centers.[6−9] The activator ions have intrinsic characteristics that contribute to the optical properties of phosphors, but it is the static and dynamic structure around the activator ions that ultimately determine luminescence performance, such as the excitation/absorption and emission wavelengths (colors) and the thermal stability of the emission efficiency (intensity). Although a large amount of host−dopant combinations have been investigated in the framework of LED conversion, only a very limited number of phosphors have actually been commercially applied because the thermal quenching behavior, i.e., the pronounced reduction in luminescence intensity at elevated temperatures (Figure 1b), remains a serious problem.

Among the most efficient phosphors for use in pc-WLEDs, particularly important are those that are based on $Ce^{3+}$-doped garnets, which typically show broadband emission spectra in the green−yellow region based on interconfigurational 4f−5d transitions of $Ce^{3+}$. In particular, this class of materials offers a remarkable flexibility in tuning the luminescence properties due to their ability to accommodate various cations and dopants.[1,2,11,12] Nevertheless, under high-power operating conditions [>1 W/chip,[13] and with the phosphor(s) in direct or near contact with the LED chip], the phosphor(s) reaches a temperature of >150 °C.[13,14] At this temperature, the vibrational dynamics at and around the activator ions has an important role. This leads to vibrationally mediated nonradiative depopulation of electronic excited states and a resulting reduction in the emission intensity of the phosphor. The thermal energy may also facilitate other nonradiative processes through thermal ionization via the conduction band (CB) of the host material and/or through excitation energy migration among the dopants to quenching sites, e.g., various kinds of defects. Additionally, when such a phosphor is contained in a LED device, the emission intensity will decrease upon heating and the emission color of the entire pc-WLED may also change. All this provides strong motivation for developing strategies for designing new, more thermally efficient and color stable phosphors with respect to the ones currently on the market. The success of any such strategy depends crucially on a thorough understanding of the

Received: December 23, 2018
Revised: March 18, 2019
Published: April 2, 2019

†This Perspective is part of the *Up-and-Coming* series.






DOI: 10.1021/acs.chemmater.8b05300
Chem. Mater. 2019, 31, 3851−3862

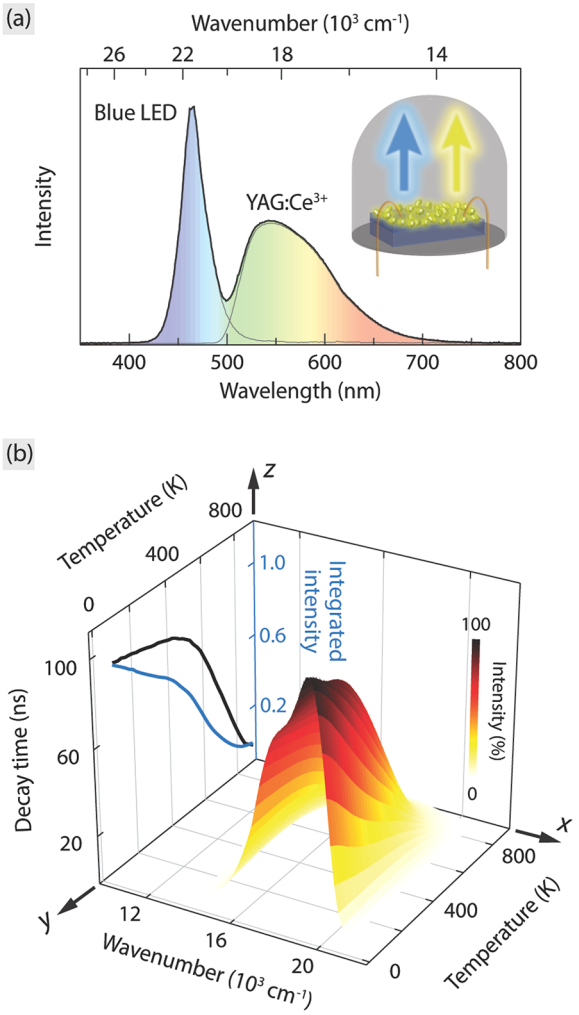


**Figure 1.** (a) Room-temperature emission spectrum of a pc-WLED device comprising a blue LED chip and a yellow phosphor ($Ce^{3+}$-doped $Y_3Al_5O_{12}$ or YAG:$Ce^{3+}$). Adapted from ref 2. Copyright 2016 Springer Nature. The inset shows a schematic of the pc-WLED device. (b) Temperature-dependent emission spectra of YAG:$Ce^{3+}$. The $y$–$z$ plane shows the integrated intensity (normalized to the intensity at the lowest temperature, 80 K) and the decay time of the emission of YAG:$Ce^{3+}$. Adapted from ref 10. Copyright 2018 Royal Society of Chemistry.

mechanism(s) of thermal quenching in materials, but this is at present not fully understood.

Here we provide an overview of our understanding of the thermal quenching of luminescence in the technologically very important class of $Ce^{3+}$-doped garnet phosphors. In particular, we summarize recent progress in determining thermal quenching mechanisms in these materials. Finally, we discuss the perspectives for future work within this field. We are hopeful that this will motivate further efforts to employ novel methodological approaches for developing a better understanding of the thermal quenching behavior of luminescent materials, to aid in the development of strategies for developing new efficient phosphors.

## 2. $Ce^{3+}$-DOPED GARNET PHOSPHORS

**2.1. Garnet Oxide Structure.** The garnet oxide crystal structure, with a general formula of $A_3B_2C_3O_{12}$, where B and C may be the same, as for $Y_3Al_5O_{12}$ (YAG), or different atoms, as for $Ca_3Sc_2Si_3O_{12}$ and $Sr_3Y_2Ge_3O_{12}$, is characterized by a 160-atom body-centered cubic unit cell (80 atoms in the primitive cell) that is assigned to the $O_h^{10}$ ($Ia\bar{3}d$) space group (see Figure 2a).[15] The A, B, and C atoms are (8-fold) dodecahedrally, (6-fold) octahedrally, and (4-fold) tetrahedrally coordinated to the O atoms of the garnet structure, respectively. The dodecahedral $AO_8$ moiety, which can be regarded as a tetragonally distorted cube, shares the coordinating O atoms with two neighboring $CO_4$ tetrahedra and four $BO_6$ octahedra.

Various combinations of the A, B, and C cations are possible, and these may be classified as follows:[11] (I) substitution of the A cation, e.g., (Y, Tb, Gd, Lu)$_3Al_5O_{12}$,[16−21] (II) substitution of the B and/or C cations, e.g., (Y, Gd)$_3Al_{5-x}Ga_xO_{12}$,[22−24] $Y_3Sc_2Al_{3-x}Ga_xO_{12}$,[25,26] and (Y, Lu)$_3Al_{5-2x}Mg_xSi_xO_{12}$,[27−29] and (III) substitution of the A (trivalent and/or divalent states), B, and C cations, e.g., (Ca, Sr)$_3$(Y, Lu, Sc)$_2$(Si, Ge)$_3O_{12}$[10,30−33] and (Y, Lu)$_{3-x}Ca_xAl_{5-x}Si_xO_{12}$.[34,35] Upon $Ce^{3+}$ substitution, the $Ce^{3+}$ ion takes the place of the A site cation in most cases, due to the similar ionic sizes and charge states of the A cation and $Ce^{3+}$. Accordingly, the local environment around $Ce^{3+}$ in the garnet structure can be described as a $CeO_8$ moiety.

**2.2. Energetics of $Ce^{3+}$ Luminescence in Garnet Phosphors.** Because the energy level structure of a free $Ce^{3+}$ ion is altered by the interaction with its nearest neighboring atoms in a host crystal, the electronic energy levels of $Ce^{3+}$ in a crystal differ greatly from those of a free $Ce^{3+}$ ion. A free $Ce^{3+}$ ion exhibits a large energy difference between the 4f ground state and the 5d excited state of 6.12 eV, but when a free $Ce^{3+}$ ion is placed in a garnet crystal, this energy difference decreases considerably.[9] The lowering of the energy gap between the 4f and 5d states, which is termed the red-shift $D$(A) for a specific host A, is predominantly dictated by two effects, the centroid shift and the crystal field splitting of the energy levels in the 5d state (see Figure 2b).[9,11,36] In comparison, the energy levels of the $Ce^{3+}$ ion in the 4f state are mainly affected by the spin−orbit coupling (s/o), which splits the 4f state into two energy levels, $^2F_{5/2}$ and $^2F_{7/2}$ (Figure 2b). For $Ce^{3+}$, the s/o is described by a one-electron (i.e., the 4f electron) interaction, which is virtually unaffected by the host crystal field surrounding $Ce^{3+}$ because the 4f electron is well-shielded by the outer filled 5s and 5p shells of electrons.[37] The centroid shift refers to a lowering of the average energy of the 5d levels of $Ce^{3+}$ (known as the barycenter) due to a decrease in the interelectronic repulsion, cf., $\varepsilon_c$ in Figure 2b, and may be determined from the (degeneracy-weighted) position of all 5d levels of $Ce^{3+}$ obtained from spectroscopic data.[38] The magnitude of $\varepsilon_c$ increases with an increase in the covalency of the bond between the $Ce^{3+}$ ion and the surrounding O anions (as may be described by the so-called covalency model) and with an increase in anion polarizability (as may be described by the so-called ligand polarization model).[38−40]

For a highly symmetric, e.g., octahedral or cubal, coordination environment, the crystal field splitting refers to the energy difference between the highest and lowest 5d levels and is again an effect of the host crystal. For a simple point charge model, it has been shown that the crystal field splitting varies as

$$\mathrm{Dq} = Ze^2r^4/6R^5 \quad (1)$$

where $Z$ is the charge of the anion, $e$ is the elementary charge, $r$ is the radius of the d orbital wave function, and $R$ is the bond


DOI: 10.1021/acs.chemmater.8b05300
Chem. Mater. 2019, 31, 3851−3862

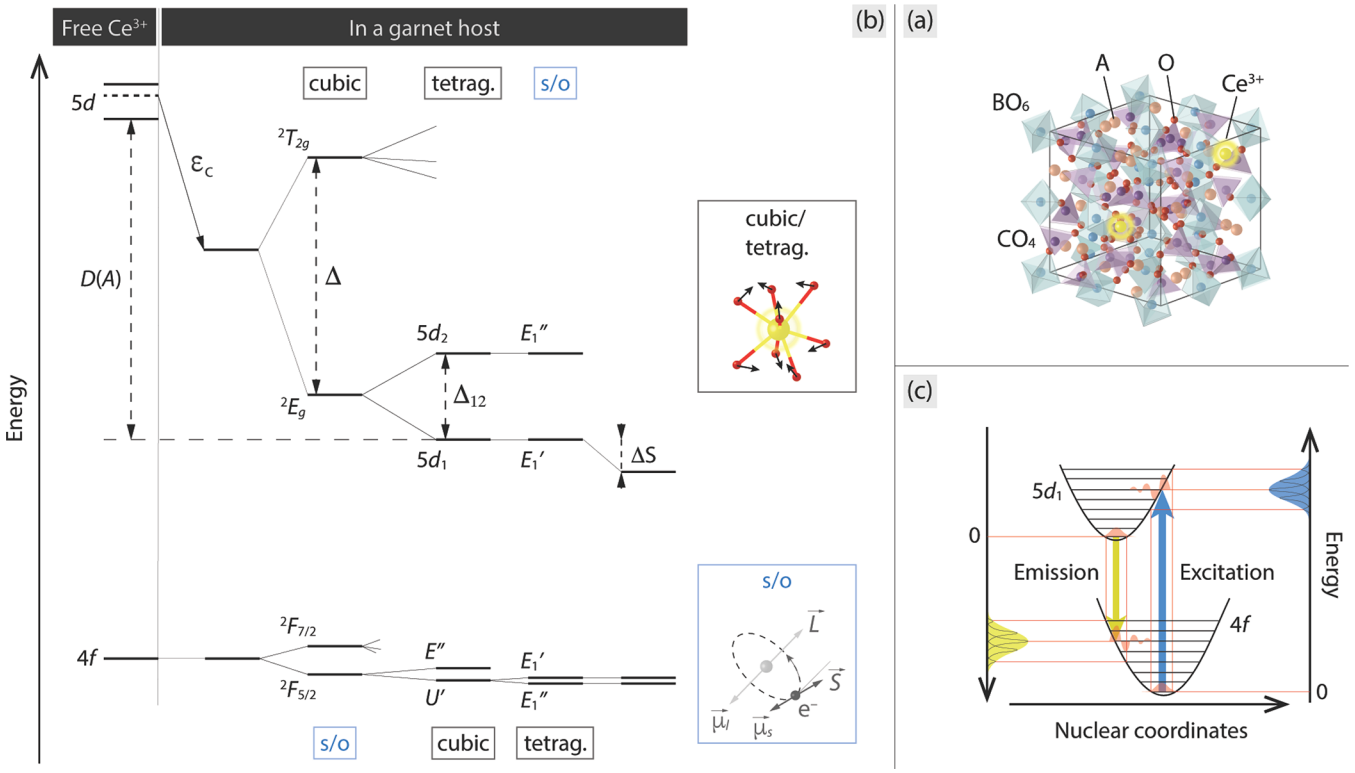


**Figure 2.** (a) Schematic illustration of the garnet crystal structure of $A_3B_2C_3O_{12}$, as doped with $Ce^{3+}$ ions on the A sites. (b) Energy diagram of the 4f ground and 5d excited electronic configurations of the $Ce^{3+}$ ions in a garnet host. Splitting of the electronic states occurs due to the cubic and tetragonal (tetrag.) symmetry of the local coordination environment of $Ce^{3+}$ and to spin−orbit coupling (s/o); see the illustration to the right ($\vec{\mu}_s$ and $\vec{\mu}_l$ represent the magnetic dipole due to the spinning electron $\vec{S}$ and the relative orbital motion of the nucleus and electron $\vec{L}$, respectively). The split energy levels related to the coordination symmetry are labeled $U'$, $E''$, $E_1'$, and $E_1''$. (c) Schematic principle of the $Ce^{3+}$ luminescence plotted in a configurational coordinate diagram in relation to excitation/absorption (blue) and emission (yellow) spectra. The parabolae represent the electronic 4f and $5d_1$ state configurations, while the horizontal lines refer to vibrational levels in each electronic state.

length from $Ce^{3+}$ to its neighboring oxygen anions.[37,41] The crystal field splitting is largest for octahedral coordination (10Dq), followed by cubal coordination [(8/9) × 10Dq = Δ (see Figure 2b)].[37,42] For a perfect cubic $CeO_8$ moiety, the 5d state splits into two levels, a doubly degenerated $^2E_g$ level and a triply degenerated $^2T_{2g}$ level. However, in the case of the $CeO_8$ moiety in a garnet structure, for which the cubic symmetry is tetragonally distorted to $D_2$ site symmetry, the $^2E_g$ level splits into two levels ($5d_1$ and $5d_2$), which is ascribed to an additional component ($\Delta_{12}$) that gives a measure of the degree of tetragonal distortion.[36] Variation of the tetragonal distortion of the $CeO_8$ moiety (as quantified by the magnitude of $\Delta_{12}$), through, e.g., the modification of the host crystal composition, thus provides a means of tuning the color of the emitted light.[22,33]

Additionally, the excitation energy arising from the 4f → $5d_1$ transition is lowered by the so-called Stokes shift ΔS (Figure 2b), which relates to vibrational relaxation and may be estimated from the difference in energy between the band maxima of the absorption/excitation and emission spectra. This vibrational (phonon) relaxation process can be understood by the use of a configurational coordinate diagram (Figure 2c), in which the potential energy curves of the $Ce^{3+}$ ion in the electronic ground and excited states are plotted against nuclear coordinates that represent the atomic (vibrational) motions localized at the luminescent center. According to the Franck−Condon principle, the electronic transitions (absorption and emission) are vertical in nature.[37] The low-temperature absorption transition shows the highest probability when it occurs from the lowest vibrational level in the ground state parabola to the one at the edge vertically above in the excited state parabola (Figure 2c) due to the largest extent of (vibrational) wave function overlapping between the initial and final states involved in the transition. Similarly, once an electron is excited to the $5d_1$ parabola, the surrounding lattice first relaxes to the lowest vibrational level of the excited state ($5d_1$) parabola before the electron is de-excited to the ground state (4f) parabola.[6,8,37] The de-excitation process, i.e., the $5d_1$ → 4f transition, leads to emission of longer wavelength light. This is followed again by vibrational relaxation to the lowest vibrational level of the 4f parabola. One may note that the vibrational relaxation to the lowest vibrational level is a 0 K behavior, whereas at temperatures of >0 K, the vibrational relaxation should follow the Bose−Einstein distribution.[37] One can conclude that the energetics of the 4f−5d optical transitions of $Ce^{3+}$ are strongly related to not only the static structural and chemical environments around the $Ce^{3+}$ ions but also the vibrational dynamics of the material. The dynamics in particular is very important in the discussion of thermal quenching behaviors, which is presented in the following sections.

## 3. THERMAL QUENCHING OF LUMINESCENCE

On a macroscopic level, in principle the easiest way to determine the response to temperature of the intensity of the emitted light is to simply measure the temperature dependence



DOI: 10.1021/acs.chemmater.8b05300
Chem. Mater. 2019, 31, 3851−3862

of the integrated emission intensity, cf., the blue curve for YAG:$Ce^{3+}$ in Figure 1b. However, because of the various factors that affect the temperature dependence of the emission intensity, such as the temperature dependence of the absorption cross section of 4f → 5d transitions and nonradiative 5d → 4f transition processes, the thermal quenching is better determined by measurements of the ratio $\eta = \tau/\tau_0$ (luminescence efficiency). Here $\tau_0$ is the radiative decay time (also known as the lifetime) of the luminescence, in the absence of quenching processes, and $\tau$ is the (temperature-dependent) experimental decay time, cf., the black curve for YAG:$Ce^{3+}$ in Figure 1b. Specifically, for many $Ce^{3+}$-doped garnet phosphors, the absorption cross section is reduced as a function of an increase in temperature. This is mainly attributed to the thermal population to the second level of the $^2F_{5/2}$ level and the fact that the transition from this level to the $5d_1$ level is symmetry forbidden (see Figure 2b).[10,16,43] In practice, $\tau_0$ may be determined from a measurement of the luminescence decay time at very low temperatures, i.e., where all vibrational modes are in their respective ground state. A useful measure in this context is the thermal quenching temperature $T_{50\%}$ (or $T_{80\%}$), which is defined as the temperature at which $\tau$ has dropped to 50% (or 80%) of $\tau_0$.

**3.1. Major Thermal Quenching Mechanisms.** On a mechanistic level, it is generally acknowledged that the thermal quenching in $Ce^{3+}$-doped phosphors exhibiting 4f−5d transitions is mainly the result of one of the three following processes or a combination thereof: (1) nonradiative 5d → 4f crossover relaxation via electron−phonon coupling, (2) thermal ionization of the 5d electron of $Ce^{3+}$ into the CB of the host lattice, followed by charge trapping at defects, and (3) thermally activated concentration quenching. These are described in the following.

*3.1.1. Nonradiative 5d → 4f Crossover Relaxation.* This mechanism refers to the process in which the excited state electron of $Ce^{3+}$ returns to the 4f ground state through vibrational relaxation. This can be explained using the quantum mechanical single-configurational-coordinate model (see Figure 3a).[44−46] The condition for nonradiative crossover relaxation is met when enough thermal energy $\Delta E$, associated with vibrational excitation at or near the $Ce^{3+}$ ion in its excited state landscape, is supplied to bring the 5d electron to the crossing point of the 5d and 4f potential energy curves in the configurational coordinate diagram. This $\Delta E$-dependent thermal quenching behavior is essentially related to the squared overlap integral of the vibrational wave functions in the 5d excited and 4f ground states under the condition of "energy resonance" between the wave functions in the two states.[44−46] The 5d → 4f crossover is followed by vibrational relaxation, which is analogous to multiphonon nonradiative relaxation occurring during 4f−4f transitions. In detail, nonradiative 5d → 4f crossover through phonon excitation (i.e., upward transition), which is promoted by a large horizontal offset between the 4f and 5d parabolae (Figure 3a), may be appoximated by an Arrhenius-dependent nonradiative transition rate: $R_{nr} = A_{nr} \times \exp^{-\Delta E/kT}$, where $A_{nr}$ is the attempt rate of the nonradiative process, $k$ is the Boltzmann constant, and $T$ is the temperature.[7,8,44,47] This leads to the relation (known as the single-barrier quenching model) $\tau = (R_r + R_{nr})^{-1} = (R_r + A_{nr} \times \exp^{-\Delta E/kT})^{-1}$, where $R_r$ $(=\tau_0^{-1})$ is the radiative transition rate that is virtually independent of temperature. $\Delta E$ depends not only on the nature of the vibrational modes in the excited state landscape of $Ce^{3+}$ but also on the difference in the local Ce−O bond length between the two electronic configurations, $|\Delta R|$. In the likely case of a harmonic oscillator, a larger $|\Delta R|$ implies a smaller $\Delta E$ and vice versa, as illustrated in Figure 3a. The fact that the 4f → 5d excitation typically leads to a decrease in the Ce−O bond length relates to the fact that when the 4f electron is excited to the 5d state the positively charged $Ce^{3+}$ nucleus becomes less shielded from the outer-shell electrons, which leads to a stronger interaction between the $Ce^{3+}$ nucleus and the O environment.[48] The magnitude of $|\Delta R|$ may be qualitatively estimated by comparing the difference in size of $Ce^{3+}$ and the host lattice ion for which it substitutes. Importantly, it relates to the so-called Huang−Rhys coupling constant $S_{HR}$,[6,37,49,50] which provides a measure of the degree of electron−phonon coupling and is defined as

$$S_{HR} = \frac{M\omega^2\Delta R^2}{2\hbar\omega} \simeq \frac{\Delta S}{2\hbar\omega} \quad (2)$$

where $\hbar$ is the reduced Planck constant, $M$ and $\omega$ are the effective ionic mass and the vibrational frequency of the coupling vibrational mode, respectively, of the $CeO_8$ moiety, and $\Delta S$ is the Stokes shift (Figure 3a). Qualitatively, the larger the $Ce^{3+}$ ion is compared to the host lattice ion, the larger the $|\Delta R|$ is.[48] This gives rise to a larger $S_{HR}$ and hence stronger electron−phonon coupling as the vibrational frequency of the coupling mode remains constant. Usually, this leads to a decrease in the quenching temperature.[6] In addition to the

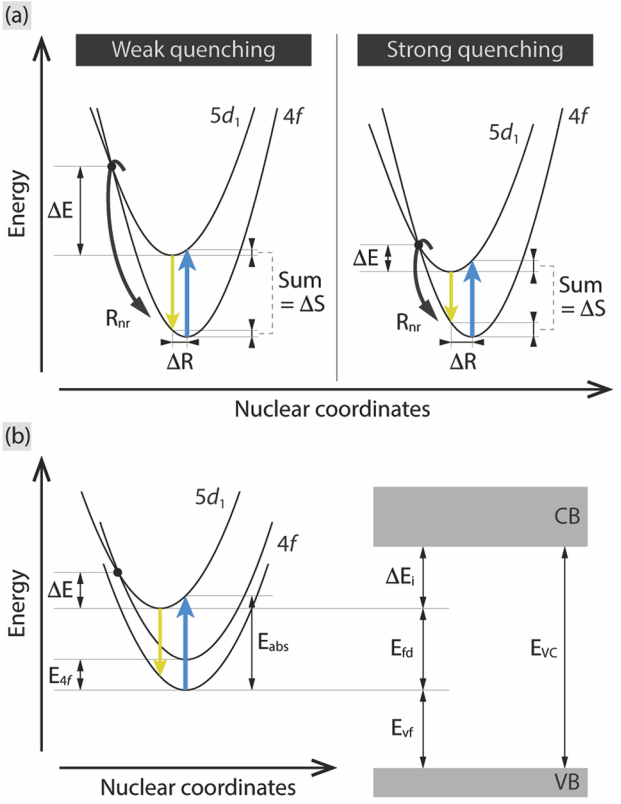


**Figure 3.** (a) Schematic illustration of nonradiative relaxation through thermally activated crossover from the $5d_1$ excited state to the 4f ground state of $Ce^{3+}$ in the cases of weak (left) and strong (right) thermal quenching. (b) Close-up of different 4f electronic potential parabolae of $Ce^{3+}$ with respect to the $5d_1$ parabola in a configurational coordinate diagram (left) and their energy positions with respect to the conduction and valence bands of the host crystal (right).



DOI: 10.1021/acs.chemmater.8b05300
Chem. Mater. 2019, 31, 3851−3862

magnitude of |Δ*R*|, the energy difference between the lowest and highest 4f levels of a lanthanide ion ($E_{4f}$), e.g., the $^2F_{5/2}$ and $^2F_{7/2}$ levels of $Ce^{3+}$ (Figure 3b), also plays a role in determining the magnitude of Δ*E*. Under the assumption that the curvature of the 4f and $5d_1$ parabolae, which reflects the stiffness of the lattice, is the same, it follows from Figure 3b that Δ*E* can be expressed as

$$\Delta E = \frac{(E_{abs} - E_{4f} - \Delta S)^2}{2\Delta S} \quad (3)$$

where $E_{abs}$ is the absorption/excitation energy of the 4f → $5d_1$ transition. This expression reveals that not only a larger Δ*S* but also a larger $E_{4f}$ leads to a smaller Δ*E* and thus to a lower quenching temperature. The effect of $E_{4f}$ on Δ*E* can be exemplified by a comparison between $Ce^{3+}$ ($E_{4f} \approx 2000$ cm$^{-1}$) and $Pr^{3+}$ ($E_{4f} \approx 22000$ cm$^{-1}$) and knowing that $Pr^{3+}$ luminescence generally exhibits a lower thermal quenching temperature as compared to $Ce^{3+}$ luminescence, in different garnet hosts, which is attributed to stronger crossover relaxation for $Pr^{3+}$ luminescence.[21,51,52]

*3.1.2. Thermal Ionization.* This mechanism refers to the process in which the 5d electron of the $Ce^{3+}$ ion is thermally promoted to the CB of the host lattice, followed by charge trapping by luminescence killer centers (e.g., substitutional impurity atoms, vacancies, antisite defects, or Ce-bound excitons)[6,52−57] (see Figure 4a). The charge trapping

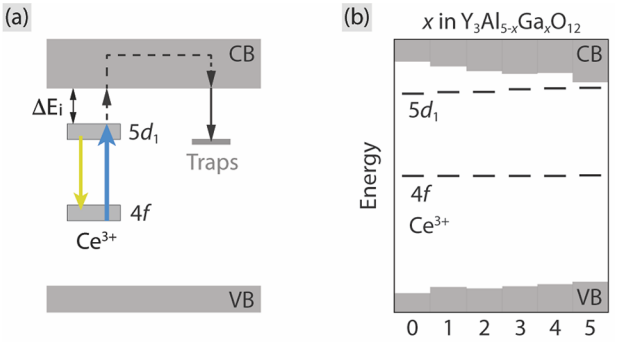


**Figure 4.** (a) Schematic illustration of the thermal quenching of $Ce^{3+}$ luminescence through thermal ionization. (b) VRBE diagram of $Y_3Al_{5-x}Ga_xO_{12}$:$Ce^{3+}$ phosphors, adapted from ref 36. Copyright 2013 Elsevier.

diminishes the luminescence, via the emission of lower-energy photons, e.g., in the form of infrared radiation,[47] or by nonradiative vibrational relaxation (i.e., energy released through heat dissipation). The trapped charges (electrons) may be as well thermally released from the defects and promoted back into the CB, which then still have a rather low probability of returning to the emitting 5d state and yielding radiative transitions, or are retrapped by the defects. This dynamical process of charge trapping and release with a variation in temperature dictates the thermal quenching.

The rate of thermal ionization $R_i$ follows an Arrhenius dependence, $R_i = A_i \times \exp^{-\Delta E_i/kT}$, where $\Delta E_i$ is the energy required to bring the 5d electron to the CB and $A_i$ is the rate coefficient.[47] Information about $\Delta E_i$ may be obtained from measurements of the temperature-dependent photoconductivity[53,58,59] and thermoluminescence.[60] Theoretically, Dorenbos developed a semiempirical, so-called chemical shift model to evaluate $\Delta E_i$.[36,61−64] On the basis of input from spectroscopic data that can be obtained from photoluminescence (PL) measurements, the chemical shift model can be used to construct the vacuum-referred binding energy (VRBE) diagram. The VRBE diagram provides an energy scheme of the absolute binding energies of the electron relative to the energies of the electron at rest, in vacuum, in the 4f and 5d electronic state configurations of all trivalent and divalent lanthanides (dopants), with respect to the energy levels of the CB and valence band (VB) of the host material. The positions of the CB and VB, which determine the band gap energy [$E_{VC}$ (see Figure 3b)], can be tuned by varying the composition of the host (bandgap engineering).[56,65−67] Together with the information about the two energies $E_{fd}$ and $E_{vf}$, as defined in Figure 3b, the value of $\Delta E_i$ can be estimated using the algebraic relation $\Delta E_i = E_{VC} - E_{fd} - E_{vf}$.[52,62,68] $E_{fd}$ is the energy of the zero-phonon transition between the lowest 4f and $5d_1$ levels, which predominantly depends on *D*(A) (Figure 2b). $E_{vf}$ is the energy difference between the lowest 4f level and the top of the VB, which is essentially determined by the energy of charge transfer from the top of the VB (mainly characterized by the 2p shell of $O^{2-}$)[69] to $Ce^{3+}$. As an example, Figure 4b shows the VRBE diagrams of $Y_3Al_{5-x}Ga_xO_{12}$:$Ce^{3+}$ (YAGG:$Ce^{3+}$) phosphors, which predict the position of the energy level of the $Ce^{3+}$ ion with respect to the CB of the YAGG host.[36] In general, a smaller $\Delta E_i$ gives rise to stronger thermal ionization quenching. When the emitting 5d state is situated within the CB, even complete quenching, due to the direct ionization and recombination of electron−hole pairs, may occur. This latter process is known as photoionization.[6]

*3.1.3. Thermally Activated Concentration Quenching.* As its name suggests, this mechanism has its roots in a decreasing thermal quenching temperature with an increase in the dopant ($Ce^{3+}$) concentration.[16,70] Specifically, this quenching mechanism depends on thermally enhanced nonradiative energy migration among dopants to luminescence killer centers (Figure 5).[47,71] Since the probability (frequency) of the energy

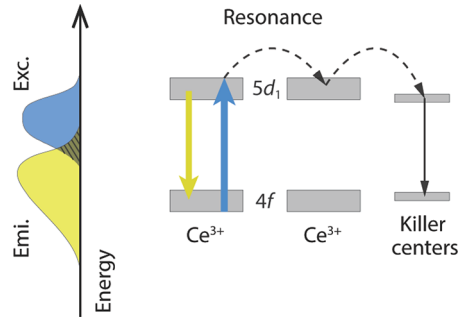


**Figure 5.** Schematic illustration of thermally activated concentration quenching of $Ce^{3+}$ luminescence. Exc. and Emi. stand for excitation and emission spectra, respectively.

transfer between different $Ce^{3+}$ ions increases with an increase in $Ce^{3+}$ concentration, the probability of trapping the excitation energy at a killer center increases, as well. The degree of resonance transfer of the excitation energy depends on the degree of overlap of the excitation (or absorption) and emission spectra (Figure 5). This overlap increases with temperature due to thermal broadening of the spectra.[37] In other words, the thermal excitation of phonon modes increases the probability of energy migration processes.[8,72] Moreover, the energy migration may also be enhanced as a result of a


DOI: 10.1021/acs.chemmater.8b05300
*Chem. Mater.* 2019, 31, 3851−3862

larger variation in the local coordination environments of the $Ce^{3+}$ ions with an increasing $Ce^{3+}$ concentration; i.e., the energy distribution of the $5d_1$ level becomes broader.[73,74] Although the existence of concentration quenching may be evident from a decrease in the thermal quenching temperature with an increase in dopant concentration, the possibility of dopant concentration-dependent crossover relaxation (as the incorporation of dopants may soften the crystal structure and hence increase the phonon population) and/or thermal ionization (as the incorporation of dopants may reduce $\Delta E_i$) must be established for a complete understanding of the quenching process.[73,75,76]

## 4. CASE STUDIES OF THERMAL QUENCHING OF THE $Ce^{3+}$ 5d → 4f EMISSION

Although there are several examples in the literature pertaining to studies that focus on understanding thermal quenching in garnet type phosphors, it is beyond the scope of this Perspective to give an exhaustive account of all the excellent work in this field. Rather, here we summarize important, novel results for thermal quenching of luminescence in $Ce^{3+}$-doped YAG and some of its variants (see Figure 6). The focus is to understand the relationship between thermal quenching and the structure and dynamics of the host.

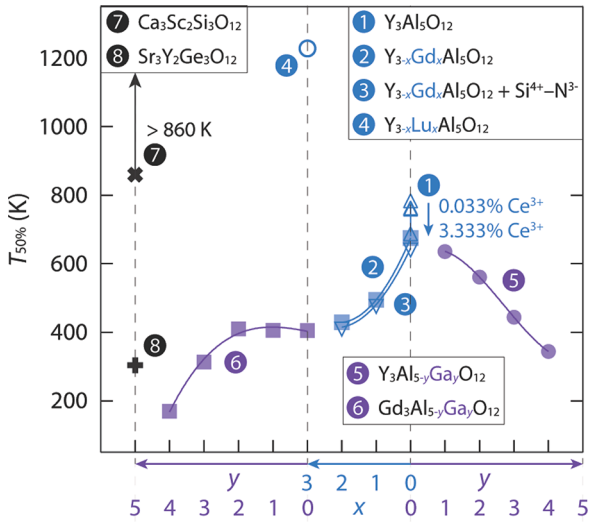


**Figure 6.** Thermal quenching temperatures of various $Ce^{3+}$-doped garnet phosphors ($T_{50\%}$), as extracted from the fits of the luminescence decay time using the single-barrier quenching model. The decay time data corresponding to the results numbered 1−8 are reproduced from refs 16 (Copyright 2009 American Chemical Society), 20 (Copyright 2019 Elsevier), 20 (Copyright 2019 Elsevier), 21 (Copyright 2013 Electrochemical Society), 23 (Copyright 2018 IEEE), 24 (Copyright 2013 American Chemical Society), 10 (Copyright 2018 Royal Society of Chemistry), and 10 (Copyright 2018 Royal Society of Chemistry), respectively.

**4.1. YAG Oxide Hosts.** *4.1.1. $Ce^{3+}$ Dopant Concentration.* The thermal quenching behavior of $Ce^{3+}$ luminescence in YAG:$Ce^{3+}$ is well-established. Bachmann et al.[16] performed a systematic study of the temperature dependence of both the intensity and decay time of the $Ce^{3+}$ emission in YAG:$Ce^{3+}$, for a wide range of $Ce^{3+}$ concentrations (between 0.033% and 3.3%). The temperature dependence of the decay time showed a strong $Ce^{3+}$ concentration dependence, with an apparent decrease in the thermal quenching temperature as a function of increasing $Ce^{3+}$ concentration (Figure 6). This difference was explained by thermally activated concentration quenching, for the higher $Ce^{3+}$ concentrations (>1%), while for the lower ones (e.g., 0.033%), $T_{50\%}$ is as high as >700 K and $\tau$ remains essentially constant up to 600 K. For the lowest $Ce^{3+}$ concentration, the $Ce^{3+}$ ions may be regarded as isolated ions; i.e., no energy transfer among neighboring $Ce^{3+}$ ions can be expected. This "intrinsic" thermal quenching may be attributed to thermally activated 5d → 4f crossover relaxation. Specifically, the phonon sideband structure suggests that local $Ce^{3+}$ vibrational modes with a frequency of ∼200 $cm^{-1}$ may be responsible for this process.[16,43] However, results from some recent studies suggest that the intrinsic thermal quenching of YAG:$Ce^{3+}$ (0.5% $Ce^{3+}$) may be predominantly associated with thermal ionization rather than crossover relaxation.[52,60]

*4.1.2. Substitution of the A Cation.* Shao et al.,[18,77] Chiang et al.,[17] and Birkel et al.[78] showed that the temperature dependence characteristics of the $Ce^{3+}$ emission intensity of YAG:$Ce^{3+}$ can be tuned by co-substitution with $Gd^{3+}$/$Tb^{3+}$ on the A sites, which lowers the quenching temperature, whereas the co-substitution with $Lu^{3+}$ on the A sites increases it. These results are in accordance with results obtained from data of the luminescence decay time,[16,20,21,24] from which $T_{50\%}$ has been extracted to be 405 K ($Gd_3Al_5O_{12}$:$Ce^{3+}$), >700 K ($Y_3Al_5O_{12}$:$Ce^{3+}$), and >800 K ($Lu_3Al_5O_{12}$:$Ce^{3+}$) (see Figure 6).

This strongly A (cation)-dependent thermal quenching temperature was initially suggested to be due to a change in $\Delta E$ for nonradiative 5d → 4f crossover quenching. This is supported by a systematic red-shift of the emission as a function of the increasing ionic size of the A cation, due to a lowering of the $5d_1$ parabola as a result of stronger crystal field splitting.[17] This is also accompanied by a larger $\Delta S$ and a smaller $\Delta E$ for the crossover quenching. In contrast, a smaller A cation implies stronger resistance against crossover quenching. This suggestion is further supported by studies of the vibrational spectra of the respective host lattice. Specifically, the high-frequency infrared (IR) and Raman spectra of the aluminum garnets $RE_3Al_5O_{12}$, where RE = Lu, Tb, or Gd, show a trend of an increasing frequency of modes in the high-frequency region (>600 $cm^{-1}$) when the ionic size of RE is smaller (see Figure 7),[73] suggesting that these modes are less readily thermally activated and the thermal quenching temperature is increased. In general, higher vibrational frequencies are congruent with a structurally more rigid compound. A high structural rigidity has been suggested to be an important criterion for not only high thermal stability toward luminescence quenching but also high quantum yield in many inorganic phosphor materials.[75,79,80] It should be noted, however, that the situation appears to be complex and the effect of the A site cation on thermal quenching has also been explained by thermal ionization. Chen et al.[81] reported that for $Gd^{3+}$ substitution, the CB is significantly lowered and $\Delta E_i$ is greatly reduced due to strong hybridization between the d orbital of $Gd^{3+}$ and the 2p orbital of $O^{2-}$. In contrast, Zhong et al.[82] found that $Lu^{3+}$ substitution results in an upward shift of the CB, which suggests an increase in $\Delta E_i$. However, $\Delta E_i$ appears to be only slightly changed according to the VRBE diagram.[36]

*4.1.3. Substitution of the B/C Cation.* Examples of studies focused on B/C cation substitutions and the concomitant effect of luminescence properties include investigations of Ga substitution in $(Y, Gd)_3Al_{5-x}Ga_xO_{12}$:$Ce^{3+}$ and $Y_3Sc_2Al_{3-x}Ga_xO_{12}$:$Ce^{3+}$ phosphors, which results in a decrease


DOI: 10.1021/acs.chemmater.8b05300
Chem. Mater. 2019, 31, 3851−3862

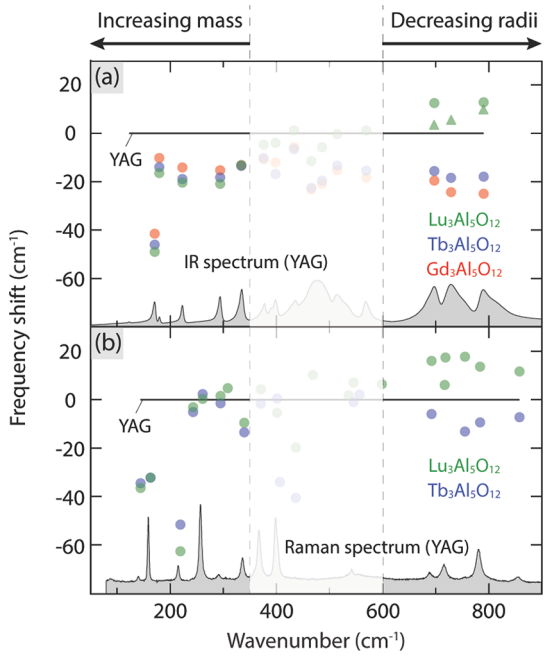


**Figure 7.** Vibrational frequency shifts of (a) IR and (b) Raman modes of the aluminum garnets $RE_3Al_5O_{12}$, where RE = Lu, Tb, or Gd, with respect to the vibrational frequencies for YAG. Adapted from ref 73. Copyright 2018 American Chemical Society.

in the thermal stability of emission intensity/decay time (Figure 6).[23−25,67,83] On the basis of photoconductivity and TL measurements, which showed the trend of a decreasing $\Delta E_i$ with an increasing level of Ga substitution (Figure 4b), this reduced thermal stability of luminescence was suggested to be due to thermal ionization. The reduction of $\Delta E_i$ is further in agreement with bandgap engineering studies,[65] which show a lowering of the CB minimum, and luminescence spectroscopy measurements,[22,84] which show an upward shift of the $5d_1$ level of $Ce^{3+}$ as a function of increasing Ga content. Finally, the statement that thermal ionization is the predominant quenching mechanism in these materials is supported by the enhanced afterglow or persistent luminescence (particularly resulting from deep traps related to other co-dopants, e.g., $Cr^{3+}$, $V^{3+}$, and $Yb^{3+}$) due to the increase in the level of charge trapping via the ionization process.[67,85−87]

*4.1.4. Substitution of Multiple Cations.* For examples of multiple-cation substitution and its effect on the thermal quenching of YAG oxide garnets, we have the cases of $CaY_2Al_4SiO_{12}:Ce^{3+}$, which is shown to exhibit thermally activated concentration quenching (when the $Ce^{3+}$ concentration increases from 0.1% to 3%),[34] and $Y_3Mg_xAl_{5-x}Si_xO_{12}:Ce^{3+}$, which exhibits a decrease in the quenching temperature upon co-substitution with $Mg^{2+}$−$Si^{4+}$ pairs.[28,88,89] Initially, this decrease in the quenching temperature for $Y_3Mg_xAl_{5-x}Si_xO_{12}:Ce^{3+}$ was associated with crossover relaxation, as inferred from an increasing Stokes shift $\Delta S$, upon the $Mg^{2+}$−$Si^{4+}$ substitution.[28,88,89] However, as pointed out by Setlur et al.,[90] $Lu_2CaMg_2Si_3O_{12}:Ce^{3+}$ exhibits a smaller Stokes shift ($\Delta S$ = 2550 $cm^{-1}$) compared to that of the thermally more stable YAG:$Ce^{3+}$ ($\Delta S$ = 2700 $cm^{-1}$), which would rather point toward another, predominant quenching process in $Lu_2CaMg_2Si_3O_{12}:Ce^{3+}$. However, the proposition of crossover quenching in $Lu_2CaMg_2Si_3O_{12}:Ce^{3+}$ is still valid when compared to $Lu_3Al_5O_{12}:Ce^{3+}$ (LuAG:$Ce^{3+}$), because LuAG:$Ce^{3+}$ shows a higher thermal stability and a smaller Stokes shift ($\Delta S$ = 2340 $cm^{-1}$).[21]

In this context, garnet hosts are, as well, known to form antisite defects (ADs), which refer to the exchange of the cation occupation between different sites and which may change the luminescence properties.[54,55,69] As an example, Seijo et al.[54] showed that the presence of ADs in the form of Y−Al site exchange in YAG:$Ce^{3+}$ leads to a blue-shift of the two lowest 4f−5d transitions. This AD-induced effect was shown to be mainly caused by upward shifts of the $5d_1$ and $5d_2$ levels,[54] whereas the overall band structure remains largely unchanged,[69] which should lead to an increased probability of thermal ionization and a decreased probability of crossover relaxation (cf. Figure 3b). Of relevance here, some studies have demonstrated that the emission efficiency of single-crystal (Y, Lu, Gd)$_3Al_5O_{12}:Ce^{3+}$ containing more ADs[91−94] exhibits less thermal quenching compared to that of the polycrystalline samples.[95−98] We infer that the ADs may have a rather weak effect on thermal quenching, as compared to other types of structural defects, which are known to promote thermally activated nonradiative processes and whose number should be significantly reduced with an increase in crystallinity.[99]

**4.2. Other Garnet Oxide Hosts.** *4.2.1. $Ca_3Sc_2Si_3O_{12}$ and $Sr_3Y_2Ge_3O_{12}$.* With regard to $Ce^{3+}$ luminescence in other garnet oxide hosts, Shimomura et al.,[30] Sharma et al.,[10] and Berezovskaya et al.[100] evidenced for $Ca_3Sc_2Si_3O_{12}:Ce^{3+}$ (CSS:$Ce^{3+}$) an excellent, intrinsic, thermal stability of luminescence up to at least 860 K (Figure 6), which is likely to be linked to a large $\Delta E_i$ of 1.36 eV (thus suppressing thermal ionization; cf., $\Delta E_i$ = 1.17 eV for YAG:$Ce^{3+}$) and high structural rigidity (thus suppressing crossover quenching).[10] Subsequent studies of CSS:$Ce^{3+}$ have mainly been focused on investigating the effect of various cation substitutions on the color of the emitted light. For example, the co-substitution of $Lu^{3+}$−$Mg^{2+}$ pairs in $Ca_{3-x}Lu_xSc_{2-y}Mg_ySi_3O_{12}:Ce^{3+}$[101] and the co-substitution of $Y^{3+}$−$Mg^{2+}$ pairs in $Ca_{3-x}Y_xSc_{2-x}Mg_xSi_3O_{12}:Ce^{3+}$[102] have shown a red-shift effect on the emission; however, the thermal stability of the emission intensity is significantly reduced due to the enhancement of crossover quenching, as inferred from the increase in $\Delta S$.

$Sr_3Y_2Ge_3O_{12}:Ce^{3+}$ (SYG:$Ce^{3+}$) exhibits a significant decrease in its luminescence decay time upon heating, starting at around 220 K ($\tau$ = 51 ns) and approaching a complete quenching of luminescence at 400 K ($\tau$ = 2 ns).[10] This very low internal stability of luminescence is attributed to a predominant thermal ionization due to a significantly smaller $\Delta E_i$ (0.45 eV) compared to those of other garnets. In comparison, SYG co-doped with $Ce^{3+}$ and $Mn^{2+}$ exhibits a quite monotonous decrease in the integrated intensity of the emission [here comprising both green (≈530 nm) emission from the $Ce^{3+}$ ions and orange (≈630 nm) emission from the $Mn^{2+}$ ions] as a function of increasing temperature.[32] Importantly, the intensity ratio of the emission from the $Ce^{3+}$ and $Mn^{2+}$ ions remains virtually constant in the investigated temperature range (41−500 K), which indicates that any plausible energy transfer processes from the $Ce^{3+}$ to the $Mn^{2+}$ ions are virtually independent of temperature and hence have no significant effects on the thermal quenching of the $Ce^{3+}$ luminescence in this material. This is rather indicative that thermal ionization of the excited electron of $Ce^{3+}$ is the dominant process.

**4.3. Garnet Oxynitride Hosts.** Nitrogen anion, $N^{3-}$, substitution on the $O^{2-}$ site, as in (Gd, Y)$_3$(Al, Si)$_5$(O, N)$_{12}:Ce^{3+}$ and $Ca_3Sc_2Si_3(O, N)_{12}:Ce^{3+}$, has been shown to


DOI: 10.1021/acs.chemmater.8b05300
Chem. Mater. 2019, 31, 3851−3862

result in a reduction in the thermal stability of the emission intensity and decay time (Figure 6).[20,103,104] This phenomenon is even more evident upon measuring the temperature-dependent decay curve of the emission monitored at the specific wavelength that is related to the $N^{3-}$ coordination environment of $Ce^{3+}$ (see Figure 8a). This reduction in

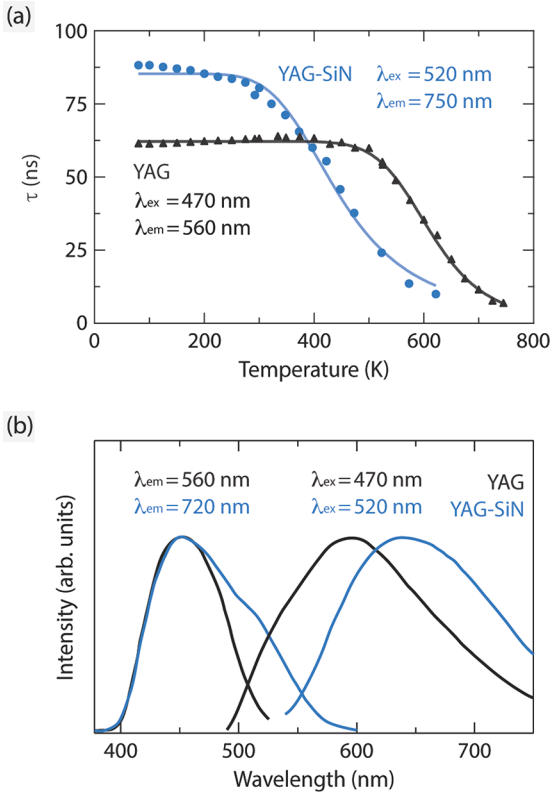


**Figure 8.** (a) Decay time of YAG:$Ce^{3+}$ and YAG:$Ce^{3+}$ co-substituted by $Si^{4+}$–$N^{3-}$ pairs (YAG-SiN:$Ce^{3+}$) as a function of temperature, adapted from ref 103. Copyright 2008 American Chemical Society. (b) Room-temperature excitation and emission spectra of YAG:$Ce^{3+}$ and YAG-SiN:$Ce^{3+}$, adapted from ref 103. Copyright 2008 American Chemical Society.

thermal stability due to $N^{3-}$ substitution can be ascribed to crossover quenching, as an effect of an increasing Stokes shift, $\Delta S$ (implying a larger $|\Delta R|$ and a smaller $\Delta E$ for crossover quenching) (see Figure 8b). The larger $|\Delta R|$, resulting from the $N^{3-}$ substitution, may be associated with the increased level of delocalization (known as the "nephelauxetic" effect[11]) of the 5d state of $Ce^{3+}$ due to the larger covalency of the Ce–N bond compared to that of the Ce–O bond.

## 5. PERSPECTIVES

From the preceding sections, it is clear that the mechanisms of thermal quenching of luminescence are a highly challenging and elusive subject, because different types of radiationless relaxation can be simultaneously competing. It is only through the combined use of new theoretical and experimental approaches, as well as the exploration of entirely new materials, that a clear mechanistic picture of thermal quenching is likely to emerge. Therefore, although YAG:$Ce^{3+}$ and its variants continue to be considered the most widely employed materials for technological applications, there are a variety of other, new and efficient phosphor families, which show interesting photoluminescence properties, or methodological approaches for developing new phosphors, some of which are highlighted here, that should be exploited further for the benefit of this field.

As a primary example of recent research findings, Kim et al.[105] reported on a new blue-emitting $Na_{3-2x}Sc_2(PO_4)_3$:$xEu^{2+}$ phosphor, which shows virtually no thermal quenching up to 200 °C. This very unusual phenomenon of zero thermal quenching originates from the ability of the phosphor to compensate for emission losses due to the polymorphic nature of the host and the energy transfer from electron–hole pairs at thermally activated defect levels to the blue-emitting 5d state of $Eu^{2+}$ (Figure 9). A similar phenomenon was recently

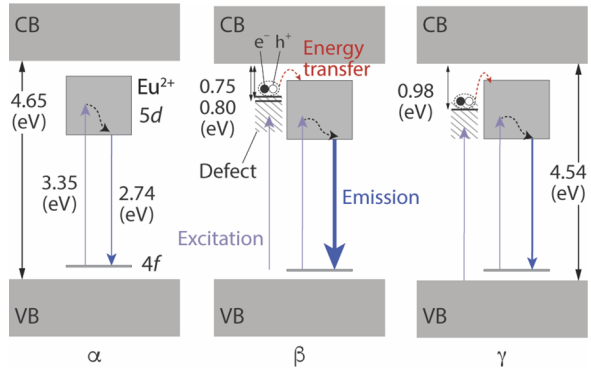


**Figure 9.** Schematic illustration of the mechanism of the zero-thermal quenching process of the $Na_{3-2x}Sc_2(PO_4)_3$:$xEu^{2+}$ phosphor, whose crystal structure changes from $\alpha$-phase (monoclinic) to $\beta$-phase (hexagonal) to $\gamma$-phase (hexagonal) with an increase in temperature. The line thickness of the emission process depicts the extent of enhanced emission intensity. Adapted from ref 105. Copyright 2017 Springer Nature.

observed in the $K_2BaCa(PO_4)_2$:$Eu^{2+}$ phosphor, which was indeed shown to exhibit a slightly increasing emission intensity with an increase in temperature from 298 to 448 K.[106] This increase in emission intensity could be explained by the recombination of $Eu^{3+}$ and electrons thermally released from defects, a process that opposes electron-trapping processes occurring as a result of thermal ionization that leads to a decrease in the emission intensity. Further examples of important results include (i) the recent discovery that the onset temperature of thermal quenching in $Ce^{3+}$-doped (Y, $Gd)_3Ga_5O_{12}$ garnets increases with an increase in applied pressure due to a pressure-induced upward shift of the CB minimum, which leads to a decrease in the level of thermal ionization,[107−109] and (ii) the discovery that the dominating thermal quenching process for the 5d → 4f emission of $Pr^{3+}$-doped $Y_3Al_{5-x}Ga_xO_{12}$ garnets can be tuned from thermal ionization to crossover quenching by controlling the position of the CB minimum from lower energy (for $x$ = 3, 4, and 5) to higher energy (for $x$ = 0, 1, and 2), respectively.[51]

The results presented above are extremely exciting and motivate further efforts to exploit polymorphic materials and/or the role of chemical and structural defects, applied pressure, and/or "phonon engineering" to deal with thermal quenching in phosphors. A particularly interesting strategy would be to turn, supposedly, bad defects (causing nonradiative charge trapping) into energetically favorable defects (compensating for the loss of emission at high temperatures). However, the nature of such "good" defects remains unclear and must be


DOI: 10.1021/acs.chemmater.8b05300
Chem. Mater. 2019, 31, 3851−3862

elucidated. Furthermore, we foresee a great opportunity for new basic science to explore the effect of different types of phonons and/or local vibrational modes on the photoluminescence properties, as little is known about the precise nature of vibrational modes involved in nonradiative and energy transfer processes in phosphors. Crucially, identifying the nature of these vibrational modes would provide a means of unraveling which local coordination environments are susceptible to thermal quenching of luminescence; such knowledge could be used for developing new design principles for designing new, efficient phosphors. Experimentally, in such studies, mode-selective vibrational excitation would be extremely useful, employing monochromatic infrared irradiation, combined with *in situ* photoluminescence measurements, which is practically achievable. Among versatile garnet phosphors, $Pr^{3+}$-doped $Y_3Al_5O_{12}$ has been regarded as a suitable candidate for this type of experiment to explicitly correlate specific vibrational modes with the crossover quenching.[21,51,52] In this context, it is also important to understand the difference in the local coordination environment of the $Ce^{3+}$ ions in the ground and excited state landscapes, especially with regard to any changes in $|\Delta R|$ (Figure 3a) as inferred by anion substitution as mentioned above. This may be studied using time-resolved techniques, such as time-resolved X-ray diffraction or absorption coupled to electronic excitation with a pulsed laser.

## 6. CONCLUDING REMARKS

Thermal quenching, in which the photoluminescence intensity diminishes with an increase in temperature, often impedes practical applications of phosphors in electronic devices and circuitry. The problem of thermal quenching becomes even more evident when one takes into account the fast development of high-power LEDs. With an increase in the amount of power consumed, the heat created by the LED will also increase, and the temperature of the phosphor layer will reach values well above today's range of 100−200 °C in available products.[13,16,110] Developing new phosphors with improved resistance to thermal quenching depends on a better understanding of the processes underpinning nonradiative relaxation mechanisms that occur at elevated temperatures. This Perspective has reviewed recent progress in understanding thermal quenching mechanisms in $Ce^{3+}$ luminescence in garnet phosphors, which are widely considered one of the most important families of phosphors for application in technological devices. Future research in this area is likely to expand and to encompass studies of both well-known and new garnet chemical compositions and will take advantage of the current development of entirely new phosphor families and/or methodological approaches. Examples of novel lines of research include the exploitation of polymorphism as well as defect structure and phonon engineering to turn the waste heat that would be generated from thermal quenching processes into photon radiation.

## AUTHOR INFORMATION


### Corresponding Author

*E-mail: maths.karlsson@chalmers.se.

### ORCID

Yuan-Chih Lin: 0000-0002-0028-7481
Marco Bettinelli: 0000-0002-1271-4241
Maths Karlsson: 0000-0002-2914-6332


### Notes

The authors declare no competing financial interest.

### Biographies

Yuan-Chih Lin received his Ph.D. in Materials Science (2018) at Chalmers University of Technology, where he has currently continued as a postdoctoral researcher. His research interests focus on unraveling structure−dynamics−property relations in inorganic phosphors, with a view toward their application in solid state lighting.

Marco Bettinelli received his Doctorate in Chemistry (1981) at the University of Parma (Parma, Italy). He was an Assistant Professor at the University of Padova (1983−1992) and an Associate Professor at the University of Salerno (1992−1993). In October 1993, he moved to the University of Verona, where he is a Full Professor of Inorganic Chemistry (since 2002) in the Luminescent Materials Laboratory, Department of Biotechnology. Recently (2015−2018), he has served as the Editor-in-Chief for *Journal of Luminescence*. His scientific interests deal with numerous aspects of luminescent materials and, in particular, the synthesis, characterization, and spectroscopic properties of crystalline, nanocrystalline, and amorphous systems containing lanthanide and transition metal ions.

Maths Karlsson received his Ph.D. in Materials Science (2007) at Chalmers University of Technology. During the years 2008−2011, he was a researcher at the European Spallation Source and Lund University (Lund, Sweden), where he, outstationed to Institut Laue-Langevin in Grenoble, France, was engaged in the development of new neutron methods. In 2011, he made the move back to Chalmers University of Technology, where he is now an Associate Professor. His scientific interests concern luminescence and luminescent materials, solid ionic conductors, and materials for hydrogen storage, often studied using techniques available at large-scale neutron and synchrotron X-ray facilities.

## ACKNOWLEDGMENTS

M.K. is grateful for financial support from the Swedish Research Council Formas (Grant 2013-1723) and Bertil & Britt Svenssons Stiftelse för Belysningsteknik.

## REFERENCES


(1) Lin, C. C.; Liu, R.-S. Advances in Phosphors for Light-Emitting Diodes. *J. Phys. Chem. Lett.* **2011**, *2*, 1268−1277.
(2) Lin, Y.-C.; Karlsson, M.; Bettinelli, M. Inorganic Phosphor Materials for Lighting. *Top. Curr. Chem.* **2016**, *374* (21), 1−47.
(3) Krames, M. R.; Shchekin, O. B.; Mueller-Mach, R.; Mueller, G. O.; Zhou, L.; Harbers, G.; Craford, M. G. Status and Future of High-Power Light-Emitting Diodes for Solid-State Lighting. *J. Disp. Technol.* **2007**, *3*, 160−175.
(4) Smet, P. F.; Parmentier, A. B.; Poelman, D. Selecting Conversion Phosphors for White Light-Emitting Diodes. *J. Electrochem. Soc.* **2011**, *158*, R37−R54.
(5) Pimputkar, S.; Speck, J. S.; DenBaars, S. P.; Nakamura, S. Prospects for LED Lighting. *Nat. Photonics* **2009**, *3*, 180−182.
(6) Blasse, G.; Grabmaier, B. C. *Luminescent Materials*; Springer: Berlin, 1994.
(7) Ronda, C. *Luminescence: From Theory to Applications*; Wiley: Weinheim, Germany, 2008.
(8) Shionoya, S.; Yen, W. M.; Yamamoto, H. *Phosphor Handbook*; CRC Press: Boca Raton, FL, 2006.
(9) George, N. C.; Denault, K. A.; Seshadri, R. Phosphors for Solid-State White Lighting. *Annu. Rev. Mater. Res.* **2013**, *43*, 481−501.
(10) Sharma, S. K.; Lin, Y.-C.; Carrasco, I.; Tingberg, T.; Bettinelli, M.; Karlsson, M. Weak Thermal Quenching of the Luminescence in the $Ca_3Sc_2Si_3O_{12}$:$Ce^{3+}$ Garnet Phosphor. *J. Mater. Chem. C* **2018**, *6*, 8923−8933.




DOI: 10.1021/acs.chemmater.8b05300
*Chem. Mater.* 2019, 31, 3851−3862

(11) Xia, Z.; Meijerink, A. $Ce^{3+}$-Doped Garnet Phosphors: Composition Modification, Luminescence Properties and Applications. *Chem. Soc. Rev.* **2017**, *46*, 275−299.
(12) Xia, Z.; Liu, Q. Progress in Discovery and Structural Design of Color Conversion Phosphors for LEDs. *Prog. Mater. Sci.* **2016**, *84*, 59−117.
(13) Tian, Y. Development of Phosphors with High Thermal Stability and Efficiency for Phosphor-Converted LEDs. *J. Solid State Light.* **2014**, *1* (11), 1−15.
(14) Setlur, A. A. Phosphors for LED-Based Solid-State Lighting. *Electrochem. Soc. Interface* **2009**, *16*, 32−36.
(15) Geller, S. Crystal Chemistry of the Garnets. *Z. Kristallogr. - Cryst. Mater.* **1967**, *125*, 1−47.
(16) Bachmann, V.; Ronda, C.; Meijerink, A. Temperature Quenching of Yellow $Ce^{3+}$ Luminescence in YAG:Ce. *Chem. Mater.* **2009**, *21*, 2077−2084.
(17) Chiang, C.-C.; Tsai, M.-S.; Hon, M.-H. Luminescent Properties of Cerium-Activated Garnet Series Phosphor: Structure and Temperature Effects. *J. Electrochem. Soc.* **2008**, *155*, B517−B520.
(18) Shao, Q.; Dong, Y.; Jiang, J.; Liang, C.; He, J. Temperature-Dependent Photoluminescence Properties of $(Y, Lu)_3Al_5O_{12}:Ce^{3+}$ Phosphors for White LEDs Applications. *J. Lumin.* **2011**, *131*, 1013−1015.
(19) Chen, Y.; Gong, M.; Wang, G.; Su, Q. High Efficient and Low Color-Temperature White Light-Emitting Diodes with $Tb_3Al_5O_{12}:Ce^{3+}$ Phosphor. *Appl. Phys. Lett.* **2007**, *91*, 071117.
(20) Asami, K.; Ueda, J.; Shiraiwa, M.; Fujii, K.; Yashima, M.; Tanabe, S. Redshift and Thermal Quenching of $Ce^{3+}$ Emission in $(Gd, Y)_3(Al, Si)_5(O, N)_{12}$ Oxynitride Garnet Phosphors. *Opt. Mater.* **2019**, *87*, 117−121.
(21) Ivanovskikh, K. V.; Ogiegło, J. M.; Zych, A.; Ronda, C. R.; Meijerink, A. Luminescence Temperature Quenching for $Ce^{3+}$ and $Pr^{3+}$ *d-f* Emission in YAG and LuAG. *ECS J. Solid State Sci. Technol.* **2013**, *2*, R3148−R3152.
(22) Wu, J. L.; Gundiah, G.; Cheetham, A. K. Structure-Property Correlations in Ce-Doped Garnet Phosphors for Use in Solid State Lighting. *Chem. Phys. Lett.* **2007**, *441*, 250−254.
(23) Venevtsev, I. D.; Khanin, V.; Rodnyi, P. A.; Wieczorek, H.; Ronda, C. Temperature Quenching of Radio- and Photoluminescence of $Y_3(Ga, Al)_5O_{12}:Ce^{3+}$ and $Gd_3(Ga, Al)_5O_{12}:Ce^{3+}$ Garnet Ceramics. *IEEE Trans. Nucl. Sci.* **2018**, *65*, 2090−2096.
(24) Ogiegło, J. M.; Katelnikovas, A.; Zych, A.; Jüstel, T.; Meijerink, A.; Ronda, C. R. Luminescence and Luminescence Quenching in $Gd_3(Ga, Al)_5O_{12}$ Scintillators Doped with $Ce^{3+}$. *J. Phys. Chem. A* **2013**, *117*, 2479−2484.
(25) Ueda, J.; Aishima, K.; Tanabe, S. Temperature and Compositional Dependence of Optical and Optoelectronic Properties in $Ce^{3+}$-Doped $Y_3Sc_2Al_{3-x}Ga_xO_{12}$ ($x$ = 0, 1, 2, 3). *Opt. Mater.* **2013**, *35*, 1952−1957.
(26) Luo, Y.; Xia, Z. Effect of Al/Ga Substitution on Photoluminescence and Phosphorescence Properties of Garnet-Type $Y_3Sc_2Ga_{3-x}Al_xO_{12}:Ce^{3+}$ Phosphor. *J. Phys. Chem. C* **2014**, *118*, 23297−23305.
(27) Katelnikovas, A.; Bareika, T.; Vitta, P.; Jüstel, T.; Winkler, H.; Kareiva, A.; Žukauskas, A.; Tamulaitis, G. $Y_{3-x}Mg_2AlSi_2O_{12}:Ce^{3+}_x$ Phosphors-Prospective for Warm-White Light Emitting Diodes. *Opt. Mater.* **2010**, *32*, 1261−1265.
(28) Maniquiz, M. C.; Jung, K. Y.; Jeong, S. M. Luminescence Characteristics of $Y_3Al_{5-2y}(Mg, Si)_yO_{12}$:Ce Phosphor Prepared by Spray Pyrolysis. *J. Electrochem. Soc.* **2010**, *157*, H1135−H1139.
(29) Ji, H.; Wang, L.; Molokeev, M. S.; Hirosaki, N.; Xie, R.; Huang, Z.; Xia, Z.; ten Kate, O. M.; Liu, L.; Atuchin, V. V. Structure Evolution and Photoluminescence of $Lu_3(Al, Mg)_2(Al, Si)_3O_{12}:Ce^{3+}$ Phosphors: New Yellow-Color Converters for Blue LED-Driven Solid State Lighting. *J. Mater. Chem. C* **2016**, *4*, 6855−6863.
(30) Shimomura, Y.; Honma, T.; Shigeiwa, M.; Akai, T.; Okamoto, K.; Kijima, N. Photoluminescence and Crystal Structure of Green-Emitting $Ca_3Sc_2Si_3O_{12}:Ce^{3+}$ Phosphor for White Light Emitting Diodes. *J. Electrochem. Soc.* **2007**, *154*, J35−J38.
(31) Pasiński, D.; Zych, E.; Sokolnicki, J. Relationship between Structure and Luminescence Properties in $Ce^{3+}$ or $Ce^{3+}$, $Mn^{2+}$-Doped Garnet Phosphors for Use in White LEDs. *J. Lumin.* **2016**, *169*, 862−867.
(32) Pasiński, D.; Zych, E.; Sokolnicki, J. $Ce^{3+}$ to $Mn^{2+}$ Energy Transfer in $Sr_3Y_2Ge_3O_{12}:Ce^{3+}$, $Mn^{2+}$ Garnet Phosphor. *J. Alloys Compd.* **2015**, *653*, 636−642.
(33) Kalaji, A.; Saines, P. J.; George, N. C.; Cheetham, A. K. Photoluminescence of Cerium-Doped $(Ca_{1-x}Sr_x)_3RE_2Ge_3O_{12}$ Garnet Phosphors for Solid State Lighting: Relating Structure to Emission. *Chem. Phys. Lett.* **2013**, *586*, 91−96.
(34) Katelnikovas, A.; Sakirzanovas, S.; Dutczak, D.; Plewa, J.; Enseling, D.; Winkler, H.; Kareiva, A.; Jüstel, T. Synthesis and Optical Properties of Yellow Emitting Garnet Phosphors for pcLEDs. *J. Lumin.* **2013**, *136*, 17−25.
(35) Katelnikovas, A.; Plewa, J.; Dutczak, D.; Möller, S.; Enseling, D.; Winkler, H.; Kareiva, A.; Jüstel, T. Synthesis and Optical Properties of Green Emitting Garnet Phosphors for Phosphor-Converted Light Emitting Diodes. *Opt. Mater.* **2012**, *34*, 1195−1201.
(36) Dorenbos, P. Electronic Structure and Optical Properties of the Lanthanide Activated $RE_3(Al_{1-x}Ga_x)_5O_{12}$ (RE = Gd, Y, Lu) Garnet Compounds. *J. Lumin.* **2013**, *134*, 310−318.
(37) Henderson, B.; Imbusch, G. F. *Optical Spectroscopy of Inorganic Solids*; Clarendon Press: Oxford, U.K., 2006.
(38) Dorenbos, P. Relating the Energy of the $[Xe]5d^1$ Configuration of $Ce^{3+}$ in Inorganic Compounds with Anion Polarizability and Cation Electronegativity. *Phys. Rev. B: Condens. Matter Mater. Phys.* **2002**, *65*, 235110.
(39) Qin, X.; Liu, X.; Huang, W.; Bettinelli, M.; Liu, X. Lanthanide-Activated Phosphors Based on 4*f*−5*d* Optical Transitions: Theoretical and Experimental Aspects. *Chem. Rev.* **2017**, *117*, 4488−4527.
(40) Dorenbos, P. 5*d*-Level Energies of $Ce^{3+}$ and the Crystalline Environment. I. Fluoride Compounds. *Phys. Rev. B: Condens. Matter Mater. Phys.* **2000**, *62*, 15640−15649.
(41) Rack, P. D.; Holloway, P. H. The Structure, Device Physics, and Material Properties of Thin Film Electroluminescent Displays. *Mater. Sci. Eng., R* **1998**, *21*, 171−219.
(42) Rogers, E. G.; Dorenbos, P. A Comparison of the Transition Metal $3d^1$ Crystal Field Splitting with the Lanthanide $5d^1$ Crystal Field Splitting in Compounds. *J. Lumin.* **2014**, *155*, 135−140.
(43) Robbins, D. J. The Effects of Crystal Field and Temperature on the Photoluminescence Excitation Efficiency of $Ce^{3+}$ in YAG. *J. Electrochem. Soc.* **1979**, *126*, 1550−1555.
(44) Struck, C. W.; Fonger, W. H. Unified Model of the Temperature Quenching of Narrow-Line and Broad-Band Emissions. *J. Lumin.* **1975**, *10*, 1−30.
(45) Struck, C. W.; Fonger, W. H. *Understanding Luminescence Spectra and Efficiency Using $W_p$ and Related Functions*; Springer: Berlin, 2012.
(46) Bleijenberg, K. C.; Blasse, G. QMSCC Calculations on Thermal Quenching of Model Phosphor Systems. *J. Solid State Chem.* **1979**, *28*, 303−307.
(47) Di Bartolo, B. *Advances in Nonradiative Processes in Solids*; Springer: New York, 1991.
(48) Blasse, G. Thermal Quenching of Characteristic Fluorescence. *J. Chem. Phys.* **1969**, *51*, 3529−3530.
(49) Huang, K.; Rhys, A. Theory of Light Absorption and Non-Radiative Transitions in F-Centres. *Proc. R. Soc. A* **1950**, *204*, 406−423.
(50) de Jong, M.; Seijo, L.; Meijerink, A.; Rabouw, F. T. Resolving the Ambiguity in the Relation between Stokes Shift and Huang-Rhys Parameter. *Phys. Chem. Chem. Phys.* **2015**, *17*, 16959−16969.
(51) Ueda, J.; Meijerink, A.; Dorenbos, P.; Bos, A. J. J.; Tanabe, S. Thermal Ionization and Thermally Activated Crossover Quenching Processes for 5*d*-4*f* Luminescence in $Y_3Al_{5-x}Ga_xO_{12}:Pr^{3+}$. *Phys. Rev. B: Condens. Matter Mater. Phys.* **2017**, *95*, 014303.
(52) Witkowski, D.; Rothamer, D. A. Emission Properties and Temperature Quenching Mechanisms of Rare-Earth Elements Doped in Garnet Hosts. *J. Lumin.* **2017**, *192*, 1250−1263.


DOI: 10.1021/acs.chemmater.8b05300
*Chem. Mater.* 2019, 31, 3851−3862

(53) Ueda, J.; Tanabe, S.; Nakanishi, T. Analysis of $Ce^{3+}$ Luminescence Quenching in Solid Solutions between $Y_3Al_5O_{12}$ and $Y_3Ga_5O_{12}$ by Temperature Dependence of Photoconductivity Measurement. *J. Appl. Phys.* **2011**, *110*, 053102.
(54) Muñoz-García, A. B.; Barandiarán, Z.; Seijo, L. Antisite Defects in Ce-Doped YAG ($Y_3Al_5O_{12}$): First-Principles Study on Structures and 4*f*−5*d* Transitions. *J. Mater. Chem.* **2012**, *22*, 19888−19897.
(55) Stanek, C. R.; McClellan, K. J.; Levy, M. R.; Milanese, C.; Grimes, R. W. The Effect of Intrinsic Defects on $RE_3Al_5O_{12}$ Garnet Scintillator Performance. *Nucl. Instrum. Methods Phys. Res., Sect. A* **2007**, *579*, 27−30.
(56) Fasoli, M.; Vedda, A.; Nikl, M.; Jiang, C.; Uberuaga, B. P.; Andersson, D. A.; McClellan, K. J.; Stanek, C. R. Band-Gap Engineering for Removing Shallow Traps in Rare-Earth $Lu_3Al_5O_{12}$ Garnet Scintillators Using $Ga^{3+}$ Doping. *Phys. Rev. B: Condens. Matter Mater. Phys.* **2011**, *84*, 081102.
(57) Ueda, J.; Aishima, K.; Nishiura, S.; Tanabe, S. Afterglow Luminescence in $Ce^{3+}$-Doped $Y_3Sc_2Ga_3O_{12}$ Ceramics. *Appl. Phys. Express* **2011**, *4*, 042602.
(58) van der Kolk, E.; Basun, S. A.; Imbusch, G. F.; Yen, W. M. Temperature Dependent Spectroscopic Studies of the Electron Delocalization Dynamics of Excited Ce Ions in the Wide Band Gap Insulator, $Lu_2SiO_5$. *Appl. Phys. Lett.* **2003**, *83*, 1740−1742.
(59) van der Kolk, E.; de Haas, J. T. M.; Bos, A. J. J.; van Eijk, C. W. E.; Dorenbos, P. Luminescence Quenching by Photoionization and Electron Transport in a $LaAlO_3:Ce^{3+}$ Crystal. *J. Appl. Phys.* **2007**, *101*, 083703.
(60) Ueda, J.; Dorenbos, P.; Bos, A. J. J.; Meijerink, A.; Tanabe, S. Insight Into the Thermal Quenching Mechanism for $Y_3Al_5O_{12}:Ce^{3+}$ Through Thermoluminescence Excitation Spectroscopy. *J. Phys. Chem. C* **2015**, *119*, 25003−25008.
(61) Dorenbos, P. Modeling the Chemical Shift of Lanthanide 4*f* Electron Binding Energies. *Phys. Rev. B: Condens. Matter Mater. Phys.* **2012**, *85*, 165107.
(62) Dorenbos, P. A Review on How Lanthanide Impurity Levels Change with Chemistry and Structure of Inorganic Compounds. *ECS J. Solid State Sci. Technol.* **2013**, *2*, R3001−R3011.
(63) Rogers, E. G.; Dorenbos, P. Vacuum Energy Referred $Ti^{3+/4+}$ Donor/Acceptor States in Insulating and Semiconducting Inorganic Compounds. *J. Lumin.* **2014**, *153*, 40−45.
(64) Rogers, E. G.; Dorenbos, P. Vacuum Referred Binding Energy of the Single 3*d*, 4*d*, or 5*d* Electron in Transition Metal and Lanthanide Impurities in Compounds. *ECS J. Solid State Sci. Technol.* **2014**, *3*, R173−R184.
(65) Vrubel, I. I.; Polozkov, R. G.; Shelykh, I. A.; Khanin, V. M.; Rodnyi, P. A.; Ronda, C. R. Bandgap Engineering in Yttrium-Aluminum Garnet with Ga Doping. *Cryst. Growth Des.* **2017**, *17*, 1863−1869.
(66) Yadav, S. K.; Uberuaga, B. P.; Nikl, M.; Jiang, C.; Stanek, C. R. Band-Gap and Band-Edge Engineering of Multicomponent Garnet Scintillators from First Principles. *Phys. Rev. Appl.* **2015**, *4*, 054012.
(67) Ueda, J.; Dorenbos, P.; Bos, A. J. J.; Kuroishi, K.; Tanabe, S. Control of Electron Transfer between $Ce^{3+}$ and $Cr^{3+}$ in the $Y_3Al_{5-x}Ga_xO_{12}$ Host *via* Conduction Band Engineering. *J. Mater. Chem. C* **2015**, *3*, 5642−5651.
(68) Dorenbos, P. The $Eu^{3+}$ Charge Transfer Energy and the Relation with the Band Gap of Compounds. *J. Lumin.* **2005**, *111*, 89−104.
(69) Muñoz-García, A. B.; Artacho, E.; Seijo, L. Atomistic and Electronic Structure of Antisite Defects in Yttrium Aluminum Garnet: Density-Functional Study. *Phys. Rev. B: Condens. Matter Mater. Phys.* **2009**, *80*, 014105.
(70) Bachmann, V.; Ronda, C.; Oeckler, O.; Schnick, W.; Meijerink, A. Color Point Tuning for $(Sr, Ca, Ba)Si_2O_2N_2:Eu^{2+}$ for White Light LEDs. *Chem. Mater.* **2009**, *21*, 316−325.
(71) Dexter, D. L.; Schulman, J. H. Theory of Concentration Quenching in Inorganic Phosphors. *J. Chem. Phys.* **1954**, *22*, 1063−1070.
(72) Shang, M.; Liang, S.; Qu, N.; Lian, H.; Lin, J. Influence of Anion/Cation Substitution ($Sr^{2+}\rightarrow Ba^{2+}$, $Al^{3+}\rightarrow Si^{4+}$, $N^{3-}\rightarrow O^{2-}$) on Phase Transformation and Luminescence Properties of $Ba_3Si_6O_{15}:Eu^{2+}$ Phosphors. *Chem. Mater.* **2017**, *29*, 1813−1829.
(73) Lin, Y.-C.; Erhart, P.; Bettinelli, M.; George, N. C.; Parker, S. F.; Karlsson, M. Understanding the Interactions between Vibrational Modes and Excited State Relaxation in $Y_{3-x}Ce_xAl_5O_{12}$: Design Principles for Phosphors Based on 5*d*−4*f* Transitions. *Chem. Mater.* **2018**, *30*, 1865−1877.
(74) Setlur, A. A.; Srivastava, A. M. On the Relationship between Emission Color and $Ce^{3+}$ Concentration in Garnet Phosphors. *Opt. Mater.* **2007**, *29*, 1647−1652.
(75) George, N. C.; Pell, A. J.; Dantelle, G.; Page, K.; Llobet, A.; Balasubramanian, M.; Pintacuda, G.; Chmelka, B. F.; Seshadri, R. Local Environments of Dilute Activator Ions in the Solid-State Lighting Phosphor $Y_{3-x}Ce_xAl_5O_{12}$. *Chem. Mater.* **2013**, *25*, 3979−3995.
(76) Chen, L.; Fei, M.; Zhang, Z.; Jiang, Y.; Chen, S.; Dong, Y.; Sun, Z.; Zhao, Z.; Fu, Y.; He, J.; Li, C.; Jiang, Z. Understanding the Local and Electronic Structures Toward Enhanced Thermal Stable Luminescence of $CaAlSiN_3:Eu^{2+}$. *Chem. Mater.* **2016**, *28*, 5505−5515.
(77) Shao, Q.; Li, H.; Dong, Y.; Jiang, J.; Liang, C.; He, J. Temperature-Dependent Photoluminescence Studies on $Y_{2.93-x}Ln_xAl_5O_{12}:Ce_{0.07}$ (Ln = Gd, La) Phosphors for White LEDs Application. *J. Alloys Compd.* **2010**, *498*, 199−202.
(78) Birkel, A.; Denault, K. A.; George, N. C.; Doll, C. E.; Héry, B.; Mikhailovsky, A. A.; Birkel, C. S.; Hong, B.-C.; Seshadri, R. Rapid Microwave Preparation of Highly Efficient $Ce^{3+}$-Substituted Garnet Phosphors for Solid State White Lighting. *Chem. Mater.* **2012**, *24*, 1198−1204.
(79) Denault, K. A.; Brgoch, J.; Gaultois, M. W.; Mikhailovsky, A.; Petry, R.; Winkler, H.; DenBaars, S. P.; Seshadri, R. Consequences of Optimal Bond Valence on Structural Rigidity and Improved Luminescence Properties in $Sr_xBa_{2-x}SiO_4:Eu^{2+}$ Orthosilicate Phosphors. *Chem. Mater.* **2014**, *26*, 2275−2282.
(80) Brgoch, J.; DenBaars, S. P.; Seshadri, R. Proxies from Ab Initio Calculations for Screening Efficient $Ce^{3+}$ Phosphor Hosts. *J. Phys. Chem. C* **2013**, *117*, 17955−17959.
(81) Chen, L.; Chen, X.; Liu, F.; Chen, H.; Wang, H.; Zhao, E.; Jiang, Y.; Chan, T.-S.; Wang, C.-H.; Zhang, W.; Wang, Y.; Chen, S. Charge Deformation and Orbital Hybridization: Intrinsic Mechanisms on Tunable Chromaticity of $Y_3Al_5O_{12}:Ce^{3+}$ Luminescence by Doping $Gd^{3+}$ for Warm White LEDs. *Sci. Rep.* **2015**, *5*, 11514.
(82) Zhong, J.; Zhao, W.; Zhuang, W.; Xiao, W.; Zheng, Y.; Du, F.; Wang, L. Origin of Spectral Blue Shift of $Lu^{3+}$-Codoped YAG:$Ce^{3+}$ Phosphor: First-Principles Study. *ACS Omega* **2017**, *2*, 5935−5941.
(83) Fu, S.; Tan, J.; Bai, X.; Yang, S.; You, L.; Du, Z. Effect of Al/Ga Substitution on the Structural and Luminescence Properties of $Y_3(Al_{1-x}Ga_x)_5O_{12}:Ce^{3+}$ Phosphors. *Opt. Mater.* **2018**, *75*, 619−625.
(84) Muñoz-García, A. B.; Seijo, L. Structural, Electronic, and Spectroscopic Effects of Ga Codoping on Ce-Doped Yttrium Aluminum Garnet: First-Principles Study. *Phys. Rev. B: Condens. Matter Mater. Phys.* **2010**, *82*, 184118.
(85) Li, W.; Zhuang, Y.; Zheng, P.; Zhou, T.-L.; Xu, J.; Ueda, J.; Tanabe, S.; Wang, L.; Xie, R.-J. Tailoring Trap Depth and Emission Wavelength in $Y_3Al_{5-x}Ga_xO_{12}:Ce^{3+}$, $V^{3+}$ Phosphor-in-Glass Films for Optical Information Storage. *ACS Appl. Mater. Interfaces* **2018**, *10*, 27150−27159.
(86) Ueda, J.; Miyano, S.; Tanabe, S. Formation of Deep Electron Traps by $Yb^{3+}$ Codoping Leads to Super-Long Persistent Luminescence in $Ce^{3+}$-Doped Yttrium Aluminum Gallium Garnet Phosphors. *ACS Appl. Mater. Interfaces* **2018**, *10*, 20652−20660.
(87) Ueda, J.; Kuroishi, K.; Tanabe, S. Yellow Persistent Luminescence in $Ce^{3+}$-$Cr^{3+}$-Codoped Gadolinium Aluminum Gallium Garnet Transparent Ceramics After Blue-Light Excitation. *Appl. Phys. Express* **2014**, *7*, 062201.
(88) Shang, M.; Fan, J.; Lian, H.; Zhang, Y.; Geng, D.; Lin, J. A Double Substitution of $Mg^{2+}$−$Si^{4+}/Ge^{4+}$ for $Al^{3+}_{(1)}$−$Al^{3+}_{(2)}$ in $Ce^{3+}$-


DOI: 10.1021/acs.chemmater.8b05300
*Chem. Mater.* 2019, 31, 3851−3862

Doped Garnet Phosphor for White LEDs. *Inorg. Chem.* **2014**, *53*, 7748−7755.
(89) Katelnikovas, A.; Bettentrup, H.; Uhlich, D.; Sakirzanovas, S.; Jüstel, T.; Kareiva, A. Synthesis and Optical Properties of $Ce^{3+}$-Doped $Y_3Mg_2AlSi_2O_{12}$ Phosphors. *J. Lumin.* **2009**, *129*, 1356−1361.
(90) Setlur, A. A.; Heward, W. J.; Gao, Y.; Srivastava, A. M.; Chandran, R. G.; Shankar, M. V. Crystal Chemistry and Luminescence of $Ce^{3+}$-Doped $Lu_2CaMg_2(Si, Ge)_3O_{12}$ and Its Use in LED Based Lighting. *Chem. Mater.* **2006**, *18*, 3314−3322.
(91) Zorenko, Y.; Voznyak, T.; Gorbenko, V.; Zych, E.; Nizankovski, S.; Dan'Ko, A.; Puzikov, V. Luminescence Properties of $Y_3Al_5O_{12}$:Ce Nanoceramics. *J. Lumin.* **2011**, *131*, 17−21.
(92) Mihóková, E.; Nikl, M.; Mareš, J. A.; Beitlerová, A.; Vedda, A.; Nejezchleb, K.; Blažek, K.; D'Ambrosio, C. Luminescence and Scintillation Properties of YAG:Ce Single Crystal and Optical Ceramics. *J. Lumin.* **2007**, *126*, 77−80.
(93) Nikl, M.; Mihokova, E.; Pejchal, J.; Vedda, A.; Zorenko, Y.; Nejezchleb, K. The Antisite $Lu_{Al}$ Defect-Related Trap in $Lu_3Al_5O_{12}$:Ce Single Crystal. *Phys. Status Solidi B* **2005**, *242*, R119−R121.
(94) Nikl, M.; Vedda, A.; Fasoli, M.; Fontana, I.; Laguta, V. V.; Mihokova, E.; Pejchal, J.; Rosa, J.; Nejezchleb, K. Shallow Traps and Radiative Recombination Processes in $Lu_3Al_5O_{12}$:Ce Single Crystal Scintillator. *Phys. Rev. B: Condens. Matter Mater. Phys.* **2007**, *76*, 195121.
(95) Arjoca, S.; Inomata, D.; Matsushita, Y.; Shimamura, K. Growth and Optical Properties of $(Y_{1-x}Gd_x)_3Al_5O_{12}$:Ce Single Crystal Phosphors for High-Brightness Neutral White LEDs and LDs. *CrystEngComm* **2016**, *18*, 4799−4806.
(96) Arjoca, S.; Víllora, E. G.; Inomata, D.; Aoki, K.; Sugahara, Y.; Shimamura, K. Temperature Dependence of Ce:YAG Single-Crystal Phosphors for High-Brightness White LEDs/LDs. *Mater. Res. Express* **2015**, *2*, 055503.
(97) Arjoca, S.; Víllora, E. G.; Inomata, D.; Aoki, K.; Sugahara, Y.; Shimamura, K. Ce:$(Y_{1-x}Lu_x)_3Al_5O_{12}$ Single-Crystal Phosphor Plates for High-Brightness White LEDs/LDs with High-Color Rendering ($R_a$ > 90) and Temperature Stability. *Mater. Res. Express* **2014**, *1*, 025041.
(98) Kang, T. W.; Park, K. W.; Ryu, J. H.; Lim, S. G.; Yu, Y. M.; Kim, J. S. Strong Thermal Stability of $Lu_3Al_5O_{12}$:$Ce^{3+}$ Single Crystal Phosphor for Laser Lighting. *J. Lumin.* **2017**, *191*, 35−39.
(99) Revaux, A.; Dantelle, G.; George, N.; Seshadri, R.; Gacoin, T.; Boilot, J.-P. A Protected Annealing Strategy to Enhanced Light Emission and Photostability of YAG:Ce Nanoparticle-Based Films. *Nanoscale* **2011**, *3*, 2015−2022.
(100) Berezovskaya, I. V.; Khapko, Z. A.; Voloshinovskii, A. S.; Efryushina, N. P.; Smola, S. S.; Dotsenko, V. P. The Effects of Temperature and Impurity Phases on the Luminescent Properties of $Ce^{3+}$-Doped $Ca_3Sc_2Si_3O_{12}$ Garnet. *J. Lumin.* **2018**, *195*, 24−30.
(101) Liu, Y.; Zhang, X.; Hao, Z.; Luo, Y.; Wang, X.; Zhang, J. Crystal Structure and Luminescence Properties of $Lu^{3+}$ and $Mg^{2+}$ Incorporated Silicate Garnet $[Ca_{3-(x+0.06)}Lu_xCe_{0.06}](Sc_{2-y}Mg_y)Si_3O_{12}$. *J. Lumin.* **2012**, *132*, 1257−1260.
(102) Pan, F.; Zhou, M.; Zhang, J.; Zhang, X.; Wang, J.; Huang, L.; Kuang, X.; Wu, M. Double Substitution Induced Tunable Luminescent Properties of $Ca_{3-x}Y_xSc_{2-x}Mg_xSi_3O_{12}$:$Ce^{3+}$ Phosphors for White LEDs. *J. Mater. Chem. C* **2016**, *4*, 5671−5678.
(103) Setlur, A. A.; Heward, W. J.; Hannah, M. E.; Happek, U. Incorporation of $Si^{4+}$−$N^{3-}$ Into $Ce^{3+}$-Doped Garnets for Warm White LED Phosphors. *Chem. Mater.* **2008**, *20*, 6277−6283.
(104) Liu, Y.; Zhang, X.; Hao, Z.; Wang, X.; Zhang, J. Generation of Broadband Emission by Incorporating $N^{3-}$ Into $Ca_3Sc_2Si_3O_{12}$:$Ce^{3+}$ Garnet for High Rendering White LEDs. *J. Mater. Chem.* **2011**, *21*, 6354−6358.
(105) Kim, Y. H.; Arunkumar, P.; Kim, B. Y.; Unithrattil, S.; Kim, E.; Moon, S.-H.; Hyun, J. Y.; Kim, K. H.; Lee, D.; Lee, J.-S.; Im, W. B. A Zero-Thermal-Quenching Phosphor. *Nat. Mater.* **2017**, *16*, 543−550.
(106) Qiao, J.; Ning, L.; Molokeev, M. S.; Chuang, Y.-C.; Liu, Q.; Xia, Z. $Eu^{2+}$ Site Preferences in the Mixed Cation $K_2BaCa(PO_4)_2$ and Thermally Stable Luminescence. *J. Am. Chem. Soc.* **2018**, *140*, 9730−9736.
(107) Lesniewski, T.; Mahlik, S.; Asami, K.; Ueda, J.; Grinberg, M.; Tanabe, S. Comparison of Quenching Mechanisms in $Gd_3Al_{5-x}Ga_xO_{12}$:$Ce^{3+}$ ($x$ = 3 and 5) Garnet Phosphors by Photocurrent Excitation Spectroscopy. *Phys. Chem. Chem. Phys.* **2018**, *20*, 18380−18390.
(108) Mahlik, S.; Lazarowska, A.; Ueda, J.; Tanabe, S.; Grinberg, M. Spectroscopic Properties and Location of the $Ce^{3+}$ Energy Levels in $Y_3Al_2Ga_3O_{12}$ and $Y_3Ga_5O_{12}$ at Ambient and High Hydrostatic Pressure. *Phys. Chem. Chem. Phys.* **2016**, *18*, 6683−6690.
(109) Kaminska, A.; Duzynska, A.; Berkowski, M.; Trushkin, S.; Suchocki, A. Pressure-Induced Luminescence of Cerium-Doped Gadolinium Gallium Garnet Crystal. *Phys. Rev. B: Condens. Matter Mater. Phys.* **2012**, *85*, 155111.
(110) Smet, P. F.; Joos, J. J. White Light-Emitting Diodes: Stabilizing Colour and Intensity. *Nat. Mater.* **2017**, *16*, 500−501.


DOI: 10.1021/acs.chemmater.8b05300
*Chem. Mater.* 2019, 31, 3851−3862